Exp. Theo. NANOTECHNOLOGY 10 (2026) 755-768 https://doi.org/10.56053/10.2.755

Remote sensing analysis: A decade of water surface changes in Lake Hamrin, Iraq

Inbethaq Mohammed Ali Abdulameer[*], *Ali Adnan N. Al-Jasim, Mahdi Haider Mahdi*

Department of physics, College of Education for Pure Science (Ibn Al-Haitham), University of Baghdad
[*]) Email: Inbethaq.m@ihcoedu.uobaghdad.edu.iq

Received 1/2/2026, *Received in revised form* 2/3/2026, *Accepted* 17/3/2026, *Published* 15/4/2026

The study of Lake Hamrin is of enormous importance in understanding changes in water levels and their impact on the local environment. It helps to clarify the role of climatic and human factors in the decline of its water resources from 2013 to 2023 in order to ensure sustainable solutions. Satellite imagery from Landsat 8 is used, and processing is performed using ArcGIS Pro and ENVI. The normalized vegetation index (NDVI) is applied to show the changes in the vegetation cover and reveal the amount of change in the surface water area of the lake. It is noted that the water area changes in one year as it increases in the rainy season and decreases in the summer, and it also varies from one year to another with the difference in the amount of rainfall. In March 2019, the largest area of the water surface of Hemrin Lake appeared, as the water surface area of the lake reached 326.87190 km² due to the increase in rainfall this year. It is noted that the lake's water area decreased during the rainy season due to the lack of rain, as the lake's water area decreased to 121.52340 km² in January 2021, while the smallest area of Hemrin Lake's water surface is reached in October 2021, as the lake's water surface area reached 28.79910 km², and the surface water area became 59.23530 km² in February 2022 due to the lack of rain during this year. In 2023, a relative increase in the lake's water area began to appear due to the return of seasonal rains this year, reaching 80.88570 km² in April, which proves to us that the change in rainfall in the region is one of the main reasons for the change in the area and water level in Hemrin Lake. The values of the earth's surface temperature are also revealed, and these values varied in the study area according to the different elements of the earth's surface and differed from one season to another and from one year to another. It is natural for the surface temperature of Hemrin Lake to rise in the summer and decrease in the winter. As the smallest area of the lake's water surface is 28.79910 km², the value of the lake's water surface temperature reached 24.9°C in October 2021. It is assumed that the area and water level of the lake decrease with the rise in temperature, but in August 2023, when the lake's water surface temperature is 31.9742°C, the lake's water surface area reached 69.75360 km². The main reasons for the decline in the water levels of Hemrin Lake are the lack of

rainfall in recent years due to climate change and the lack of water releases from Lake Darbandikhan due to the lack of water coming to it from the Iranian side, as well as the significant decline in the waters of the Alwend River due to its interruption by the Iranian side due to the construction of dams and the change in its course and the cessation of its flow in the summer.

Keywords: Lake Hamrin; Climate Change; Water Level; NDWI; NDVI.

1. INTRODUCTION

Most studies focused on developments in nanotechnology. The bodies of water that spread the surface of the Earth having nanoparticles are considered one of the important phenomena of the environment and human life [1]. Many studies and measurements have been conducted for these bodies of water using remote sensing techniques in addition to geographic information systems. Lakes are one of the important bodies of water, as they play a role in regulating the hydrological cycle. Environmentally, it has economic and tourism importance for humans in terms of use for agricultural purposes, agricultural fishing, freshwater sources, and electric power generation. Any changes that occur in the lake result from climatic changes and human activities that have a direct impact on the environment and human life, and remote sensing techniques can help in monitoring these changes and in managing lake water [2, 3]. Water is necessary to maintain the balance of the environment and provide all human needs, especially in countries that are characterized by semidry or dry weather, such as Iraq, which is affected in the event of a shortage in the amount of water. The presence of water is an essential factor in distributing population density, which depends mainly on agriculture and in controlling economic activity because it is the basis for providing people with the food they need [4]. In recent years, Iraq has been exposed to the drought of many lands due to the lack of water imports from the source and the decrease in rainfall levels by a significant percentage of up to 40% from the normal rate. Water levels in the main rivers in Iraq decreased significantly due to the Turkish dam project on the Tigris and Euphrates Rivers and the irrigation projects and dams that are constructed on the tributaries of the Tigris River that originate from Iranian territory, such as the Alwend River, whose direction is changed towards the Iranian side [5-7]. Studies are conducted on the water bodies and lakes of Iraq, relying on remote sensing data, these studies are showed that the influence of human and natural activities factors is the direct cause of the changes occurring in the surface areas of lakes during recent years, and these changes are mainly related to water policies [8, 9]. Studying the climate and weather conditions of a particular place is important over a long period of time, and monitoring the weather on a daily, seasonal and annual basis depends on climate change over time, as climate changes are linked to social living standards and technological development in countries on the one hand and the effects that appear on the environment on the other hand, in particular on Developing countries in Africa, Asia and South America are seriously affected by climate change, so modern studies and research should be greatly interested in studying climate change supported by new nanotechnology . The continuous rise in climate temperature and the increase in human activities have led to the drying up of many lakes and oases on Earth and other environmental problems to a change in the size and area of lakes and water reservoirs, especially during recent years. Therefore, the variation in measuring the depths and areas of lake water and reservoirs is a measure of environmental changes from place to place another and from time to time [10, 11]. The lack of water in Diyala (eastern Iraq) has become a threat to the region in recent years. As a result, the levels of the most famous lake in Diyala Governorate, known as Hemrin Lake, have decreased, which is the main source for supplying the governorate with water and for irrigating many agricultural lands, as the water storage capacity in Hemrin Lake reaches to (3.76 billion cubic metres), and times of floods may pose a danger to populated areas and neighboring agricultural lands that are located below the lake, causing greater destruction to neighboring areas. Sometimes flooding leads to loss of life, so the local administration is required in times of drought and floods to take the necessary measures to confront the changes that occur in the lake levels [12]. The

decline and scarcity of water resources in the countries of the Middle East and the increase in demand for them appeared in the 1970s, which led to negative effects on economic development, prosperity and political stability in the region. Iraq is not among the neighboring countries that suffered from water scarcity due to its possession of the Tigris and Euphrates rivers. There are many natural tributaries and reservoirs represented by lakes and marshes, in addition to the artificial reservoirs that are formed behind many of the dams built in the past decades. In the first half of the twentieth century, interest began in building irrigation systems and controlling flood times in Iraq to protect the capital, Baghdad, and other major cities from floods [13].With the development of the field of satellite image processing, more accurate data is obtained and a study is presented in estimating the percentage of moisture in the soil, classifying the components of the study area, and determining the uses of agricultural land, locations of natural vegetation, and soil types. As well as residential and industrial areas, identifying areas most exposed to floods, and taking the necessary measurements to avoid such disasters by identifying locations necessary to build dams according to specific standards. Remote sensing applications can be used to monitor the flow of rivers. It also helps in providing appropriate designs for future water control projects to help in Storing excess flood water and reusing it again during dry seasons [14].

The study aims to monitor changes in the water area of Hemrin Lake during the recent ten years. Some years have witnessed a significant decrease in the lake's water area, and satellite images showed variation in the lake's water area from season to another and from year to year. Scope of the Project, this study analyzes the changes in the water level of Hemrin Lake between 2013 and 2023 using remote sensing techniques, aiming to identify the environmental and hydrological factors affecting the lake, primarily the decline in rainfall and reduced water releases from upstream sources.

1.2 Study Area

Hemrin Lake is located in Diyala Governorate on the Diyala River in central Iraq, 50 km northeast of Baqubah, 120 km northeast of Baghdad, between latitudes 44° 53′ 26.16' - 45° 07′ 28.03″ and 34° 04′ 24.75″ - 34° 19′ 12.74″, The maximum length of the lake is 50 km, its maximum width is 17 km, and its height above sea level is about 107.5 m. The total area is 489 km², and the carrying capacity of Hemrin Lake is about 4.61 billion m³. Sometimes, the changes in the surface water area of Hemrin Lake affect its shape. Hemrin Lake is an artificial lake located behind the Hemrin Dam. The Hemrin Dam is constructed in 1976 on the Diyala River, which is a tributary of the Tigris River, and began operating in 1981 for irrigation, flood control, and hydroelectric power generation. Its greatest water area is recorded in 1988 when the surface water area reached 358.38 km². The main source of the lake's water is from the Darbandikhan reservoir, which is about 117 km from Hemrin Lake, as well as from the source and tributaries of the Diyala River and from the Al-Wand River, which flows from within Iranian territory [15]. The location of Lake Hamrin in Iraq is shown in Figure 1.

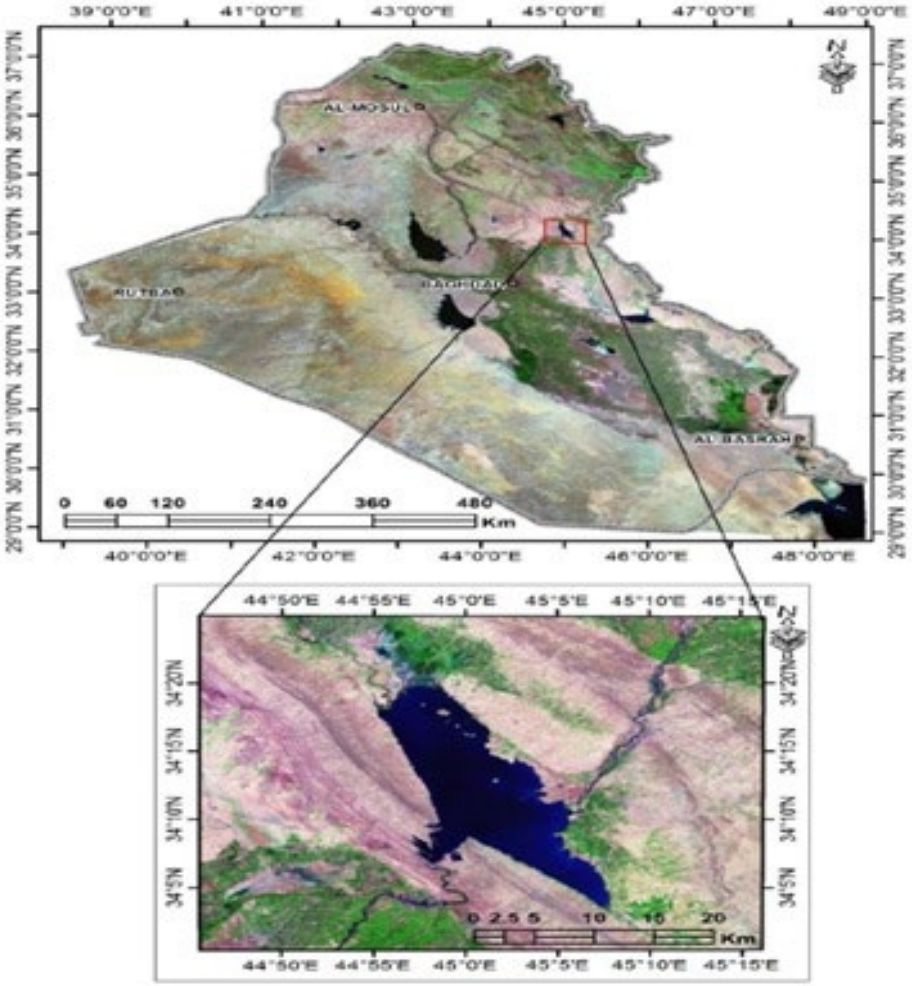

Figure 1 Location of Lake Hamrin in Iraq [16].

2. METHODOLOGY

2.1 The software

Images are downloaded from the 30-meter ground-resolution Landsat OLI satellite of the United States Geological Survey (USGS) during specific periods from 2013 to 2023 respectively, to detect changes in the waters of Hemrin Lake [17]. The images are processed and changes in the area of the lake's water bodies are detected by using Normalized Difference Vegetation Index **(**ENVI 3.5) and Quantitative Geographic Information Systems (24.3 QGIS) software.

2.2 Image processing

The ENVI program is used to correct the downloaded images of the study area based on the image data archived in the UTM file. Due to the large area of the downloaded images, the area is subtracted by specifying new coordinates to cut the image [(484455 E, 3835905 N (UP)], [539295 E, 3761865 N (DON)]. The visible digital number (DN) value is converted into reflectance spectra to show the features of the study area with high clarity and great accuracy through the reflectance properties of each spectral band to display the components of the earth's surface using the following equation [18].

$$P\lambda = (Mp * Qcal + Ap) / \sin\theta \quad (1)$$

Pλ, = radiative reflection (m2* sr * m), Mp= reflectance multiplicative of each band, Qcal = represents pixel value in DN, Ap = reflectance additive scaling for the bands, (θ) = solar elevation angle **.**

2.3 Spectral indicators used in the study
2.3.1 Normalized difference vegetation index (NDVI)

The vegetation index is used to show the density of the vegetation on the ground and distinguish between modern and ancient plants depending on the frequency of the red rays and the nearby infrared, and the areas free from the plant absorb infrared radiation. Healthy plant leaves appear green because they contain chlorophyll, which efficiently absorbs red and blue wavelengths while reflecting green wavelengths, in addition to a good reflection of infrared rays near the cellulose substance found in the branches of the plant, which makes it look bright compared to unhealthy plants. Red and blue wavelengths, so they look yellow in the fall season. The NDVI index has positive values between -1 and 1, with an NDVI < 0 indicating cloud or water; the vegetable cover gives the values of its range (0.8-0.3). As for the shrubs and herbs, it gives values (0.2 - 0.3). NDVI values are calculated from the following equation [19,20].

NDVI = band (NIR) −band (Red)/ band (NIR) +band (Red) (2)

where the band (NIR) = the fifth band of Landsat 8 (near 0.85-0.88) µm, the (Red) band = the second band of Landsat 8 (0.64-0.67) µm.

2.3.2 Land surface temperature

It is a measurement of the land surface temperature (LST) and is an important variable to evaluate for detecting surface heat, as LST depends on the wave of thermal radiation emitted from the surface to measure temperatures between the Earth's surface and the atmosphere. Thermal parameters for the research area are obtained from data archived in the (MTL) file in the geostationary satellite sensor. It is the best source to provide us with the information we need to estimate the LST for large areas in distance learning completely throughout the year [. Several steps are applied to obtain LST values with high spatial resolution over different periods, which include [21,22].

1. The radiative reflection (Lλ) from Band (10) is found by applying the following equation.

Lλ= ML* Qcal +AL (3)

Where L λ= is radiative reflection (m2 * sr * m), ML = is Standardization factor specific to each package, Qcal = the numeric value of the pixel, AL = Correction factor

2. The brightness temperature is measured from the following equation [21,22].

TB = (K2 / (Ln (K1/ Lλ+1))-273.15 (4)

where TB = the brightness temperature, K1= Conversion factor constant (thermal band 10), K2 = Transformation factor steady (thermal band 10).
3. The amount of NDVI is extracted from the equation (2).
4. The value of percentage of the vegetation is found by applying the equation [21].

Pv= ((NDVImax-NDVImin)/ (NDVImax-NDVI min)) ^{2} (5)

where Pv = The percentage of vegetation cover, NDVImin It is the lowest value of NDVI for soil exposed pixels and NDVImax It is the highest value of NDVI for a healthy vegetable pixel
5. The amount of Emissivity is obtained from the following equation [23,24].

$$E = 0.004 * Pv + 0.986 \quad (6)$$

where E =the Emissivity correction factor is a constant value.
6. Land surface temperature values are extracted from the following equation [25] [26].

$$LST=TB / (1+ (\lambda *TB/P) *Ln (E)) \quad (7)$$

where LST =Land Surface Temperature, $\boldsymbol{\lambda}$= wavelength of Band 10 = 10.8 μm P= (14388) Fixed value $(h * c)/k_B$ (h= Planck constant, $K_{B=\text{Boltzmann}}$ constant, c = Light velocity)

2.4 Satellite images data

Archived images of the study area are downloaded from the Landsat (8) satellite from 2013 to 2023. The study focused on two periods of each year, namely the rainy season and the dry season. The satellite images amounted to 22 images at a rate of two images for each year of the study period. They included some of the required data as shown in Table 1.

Table 1 Satellite data covering the study area for the period 2013–2023.

No	Satellite	Sensor Type	Date Acquired	Time	Path/row
1	Landsat 8	OLI_TIRS	2013-04-02	07:38:13.8385100Z	169/36
2	Landsat 8	OLI_TIRS	2013-08-11	07:35:14.0149010Z	168/36
3	Landsat 8	OLI_TIRS	2014-03-07	07:33:47.6481810Z	168/36
4	Landsat 8	OLI_TIRS	2014-07-29	07:33:09.5833310Z	168/36
5	Landsat 8	OLI_TIRS	2015-01-21	07:33:11.7086550Z	168/36
6	Landsat 8	OLI_TIRS	2015-08-17	07:32:57.1917840Z	168/36
7	Landsat 8	OLI_TIRS	2016-03-12	07:33:04.6458660Z	168/36
8	Landsat 8	OLI_TIRS	2016-10-06	07:33:30.2376650Z	168/36
9	Landsat 8	OLI_TIRS	2017-02-27	07:33:05.6828150Z	168/36
10	Landsat 8	OLI_TIRS	2017-08-06	07:33:13.3950760Z	168/36
11	Landsat 8	OLI_TIRS	2018-03-18	07:32:46.2309090Z	168/36
12	Landsat 8	OLI_TIRS	2018-10-28	07:33:07.6199940Z	168/36
13	Landsat 8	OLI_TIRS	2019-03-21	07:32:48.3965790Z	168/36
14	Landsat 8	OLI_TIRS	2019-10-15	07:33:36.9999310Z	168/36
15	Landsat 8	OLI_TIRS	2020-03-23	07:33:00.7208240Z	168/36
16	Landsat 8	OLI_TIRS	2020-09-15	07:33:28.2401270Z	168/36
17	Landsat 8	OLI_TIRS	2021-01-05	07:33:28.6589760Z	168/36
18	Landsat 8	OLI_TIRS	2021-10-04	07:33:36.1755670Z	168/36
19	Landsat 8	OLI_TIRS	2022-02-09	07:33:20.3811560Z	168/36
20	Landsat 9	OLI_TIRS	2022-09-13	07:33:29.7590749Z	168/36
21	Landsat 8	OLI_TIRS	2023-04-17	07:32:45.6135859Z	168/36
22	Landsat 8	OLI_TIRS	2023-08-23	07:33:12.8830180Z	168/36

4. RESULTS AND DISCUSSION

The Quantitative Geographic Information Systems (QGIS) software is used to determine the area and temperature of three samples in the study area: the water surface of Hamrin Lake, vegetation, and soil. Additionally, the link (https://power.larc.nasa.gov/data-access-viewer) is used to measure the annual precipitation in the study area, as presented in Table 2.

Table 2 Empirical results of the study area over the period 2013–2023.

no	Data Acquired	Area Lake(km^2)	Area Solid (km^2)	Area Vegetation (km^2)	Temperature Water lake(℃)	Precipitation (mm)
1	2013-04-02	197.34030	3091.00140	775.87920	18.8287	195.12
2	2013-08-11	149.70510	3702.40290	212.02560	28.9369	
3	2014-03-07	230.33880	2355.30450	1478.30670	16.0697	221.48
4	2014-07-29	116.43120	3678.31800	269.32680	28.1962	
5	2015-01-21	162.78480	3207.05280	693.89640	8.82830	263.67
6	2015-08-17	88.07850	3731.44680	244.68930	28.2154	
7	2016-03-12	245.88720	1600.90290	2217.42360	17.3422	195.12
8	2016-10-06	295.62300	3422.19960	346.24710	23.3397	
9	2017-02-27	231.28690	3206.83860	626.05400	15.4365	137.11
10	2017-08-06	208.88910	3618.20970	236.64780	29.0490	
11	2018-03-18	239.16110	3126.47100	698.58880	16.9933	437.7
12	2018-10-28	143.01900	3657.34800	263.47500	21.8422	
13	2019-03-21	326.87190	721.69560	3015.62730	14.5543	326.95
14	2019-10-15	283.43160	3450.66030	330.12090	22.8099	
15	2020-03-23	221.05260	2189.98620	1652.92830	15.4574	195.12
16	2020-09-15	150.21630	3640.44240	273.49380	27.4679	
17	2021-01-05	121.52340	3414.20130	528.45930	9.7639	89.55
18	2021-10-04	28.79910	3866.91570	168.33690	24.9176	
19	2022-02-09	59.23530	3549.90960	454.95810	12.0989	174.91
20	2022-09-13	35.07030	3856.45230	172.59570	21.2061	
21	2023-04-17	80.88570	2755.94400	1227.29940	21.5162	280.14
22	2023-08-23	69.75360	3816.18720	178.11900	31.9742	

The Normalized Difference Vegetation Index (NDVI) is adopted to show the elements of the study area to determine the water surface area of Hemrin Lake and calculate its area for the period between 2013-2023 by applying an equation 2, as shown in Figure 2.

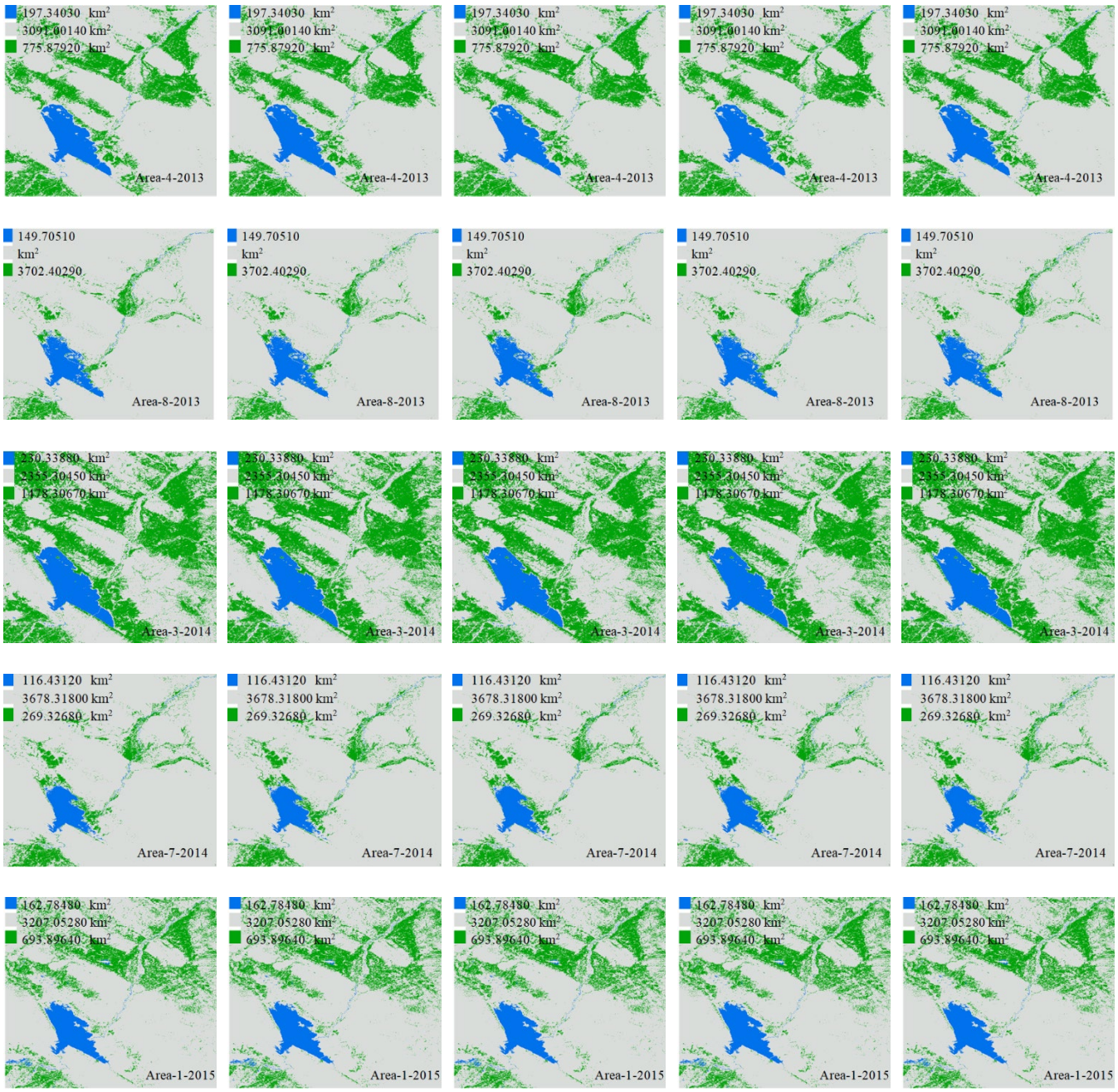

Figure 2 NDVI of the study area during the period 2013–2023.

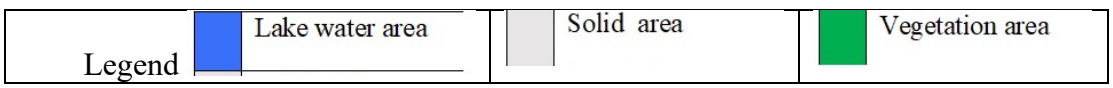

After applying equation (2) to calculate the national vegetation index, it is noted that the water area changed in one year, as it increased in the summer and decreased in the rainy season, and it also varied from year to year with the difference in the amount of rainfall. In the rainy season exclusively, and in March 2019, the largest area of the water surface of Hemrin Lake appeared, as the surface area of the lake's water reached 326.87190 km² due to the increase in rainfall this year and the recovery of the Diyala River in the upper part of the lake, the main feeder of the lake, as well as the Al-Wand River, which feeds the Diyala River northeast of the lake, and also the rainwater that collects in the valleys within the study area that flow into the Diyala River from both sides [27]. It is noted that the lake's water area decreased in the rainy season due to the lack of rain, as the lake's water area decreased to

121.52340 km² in January 2021, while the smallest area of the water surface of Hemrin Lake is reached in October 2021, as the surface area of the lake's water reached 28.79910 km² and the surface water area became 59.23530 km² in February 2022 due to the lack of rainfall during this year [28]. As for 2023, a relative increase in the lake water area began to appear due to the return of seasonal rains this year, as it reached 80.88570 km². This proves to us that the change in rainfall in the region is one of the main reasons for the change in the area and water level in Hemrin Lake, as shown in Figures 3 and 4.

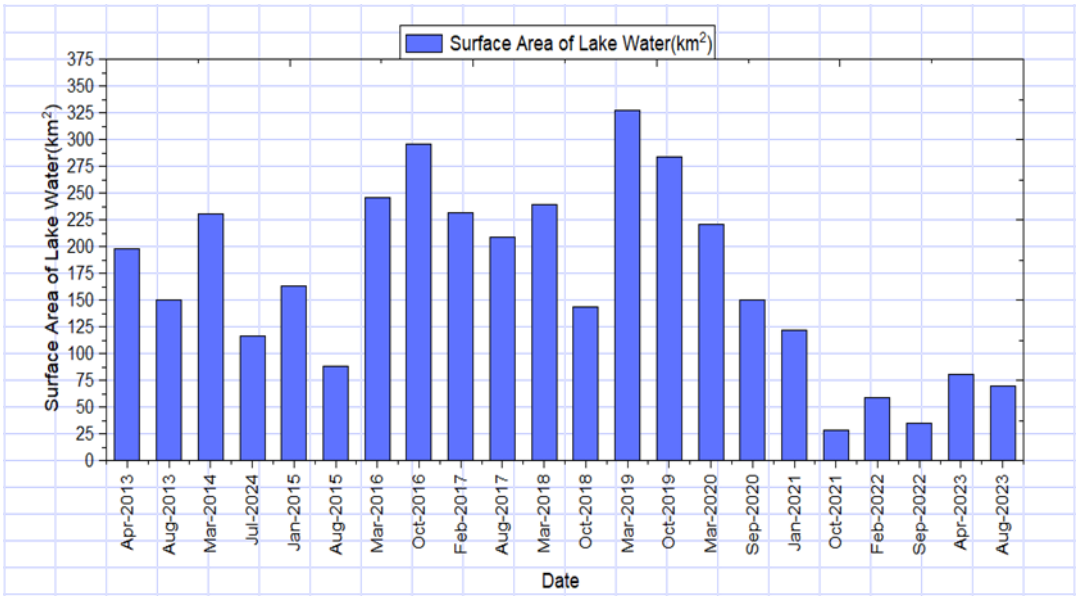

Figure 3 The variation in the surface area of Hemrin Lake water in the period 2013-2023.

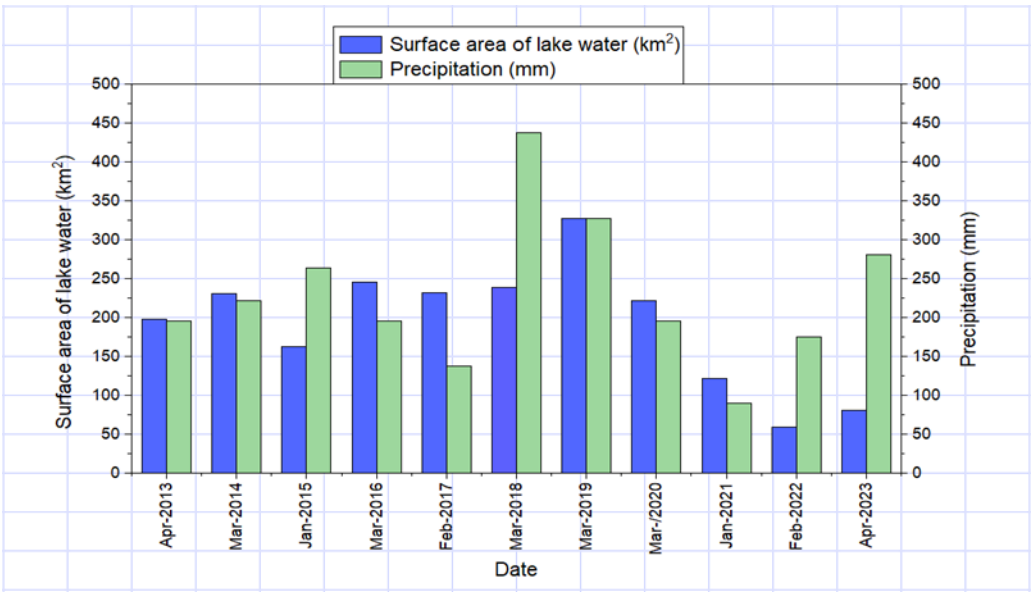

Figure 4 Variation of lake surface area with precipitation during the rainy season 2013–2023.

Equation 7 is applied to show the temperature of three elements in the study area: the lake water surface, plants, and soil in two regions, for the period between 2013 and 2023, as shown in Figure 5.

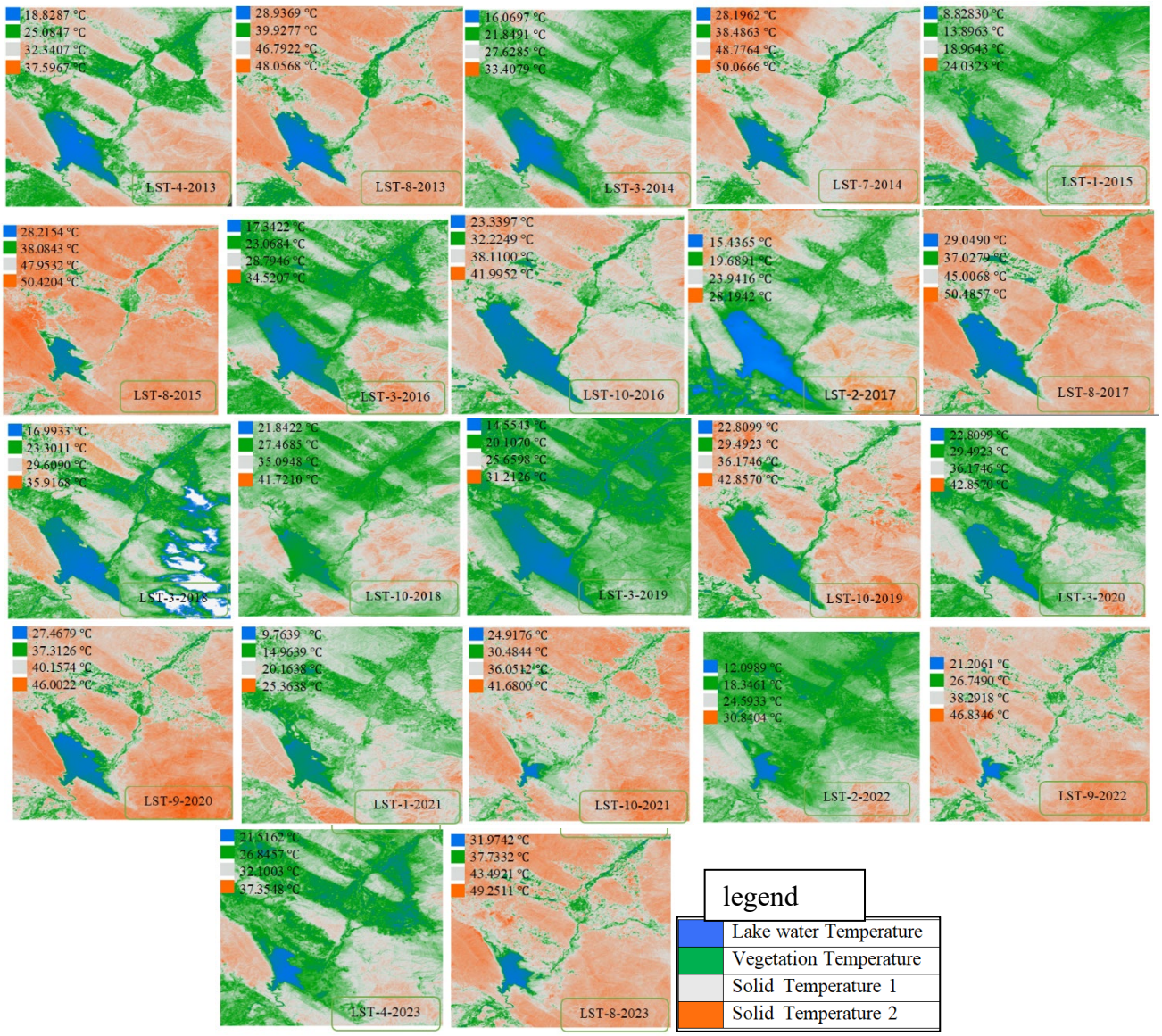

Figure 5 Land surface temperature LST for the study area during 2013-2023.

By applying equation 7, the values of the land surface temperature LST are revealed. These values varied in the study area according to the different elements of the earth's surface and varied from one season to another and from one year to another. It is natural for the surface water temperature of Hemrin Lake to rise in the summer and decrease in the winter, as the smallest area of the lake's water surface is 28.79910 km^2 and the value of the surface temperature of the lake's water reached 24.9 ℃ in October 2021 [29]. It is assumed that the area and level of the lake's water will decrease with the temperature rise, but in October 2019, the temperature value is 22.8℃ , and the surface area of the lake's water reached 283.43160 km^2. In August 2023, when the surface temperature of the lake's water is 31.9742 ℃ , the surface area of the lake's water reached 69.75360 km^2. This mean that the change in temperature is not the main reason for the decrease in the lake's water level, as illustrated in Figures 6 and 7.

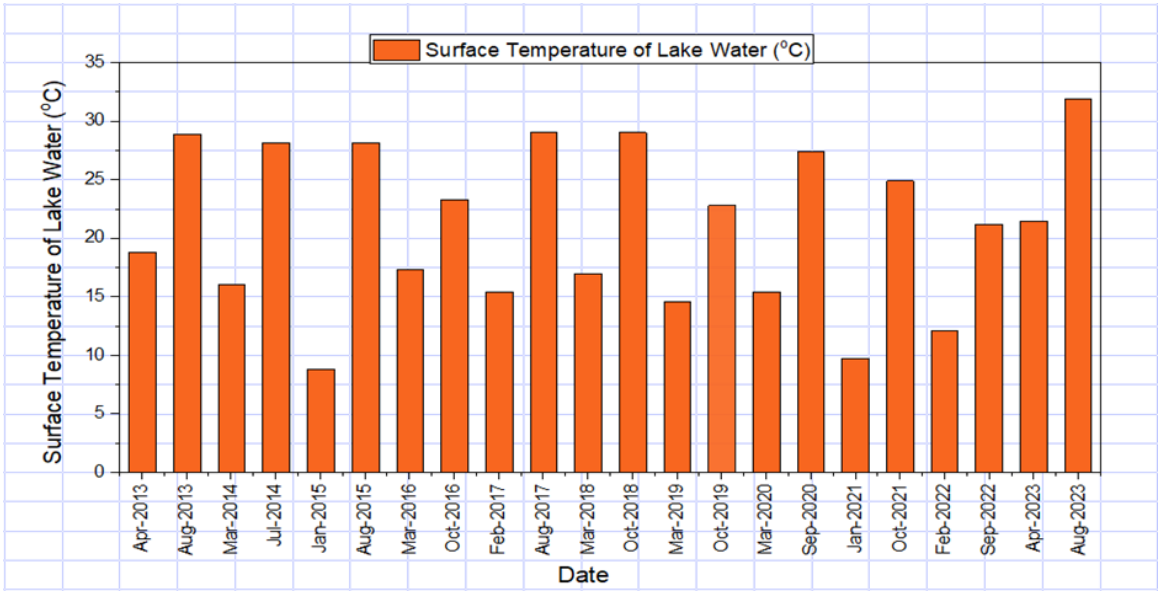

Figure 6 Variation in Hemrin Lake surface temperature during 2013–2023.

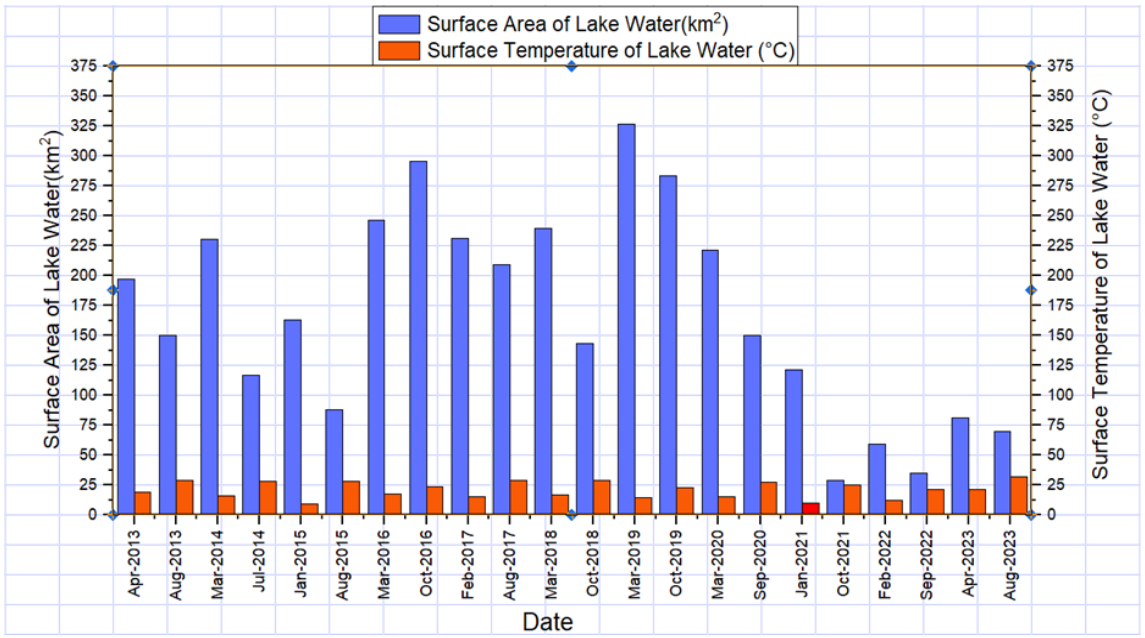

Figure 7 Variation in Lake surface area with changes in surface temperature during 2013–2023

4. CONCLUSIONS

The main conclusions drawn from this research concerning the study area are as follows

1. Climate change in the study area is a major cause of the variation in water levels of Hemrin Lake.
2. The significant decrease in the amount of rainfall in the study area and the surrounding lands that contain rivers and valleys that feed Hemrin Lake is the main reason for the decrease in water levels of the lake.
3. The rise in temperatures has an effect on the variation in water levels of the lake, but it is not a major cause.
4. The construction of dams on the rivers that flow into the Diyala River, the main water feeder of the lake, by the neighboring country of Iran to Iraq from the east, and changing the course of some of

them, such as the Alwend River, is a major reason for the decrease and drying up of large areas of the lake's water.

Given the findings of this study, it is recommended that the waters of Lake Hamrin be preserved by implementing sustainable water management strategies, taking into account climate change in the region and reduced water flow from upstream sources. Regularly monitor the lake using satellite imagery and analyze the Normalized Difference Vegetation Index (NDVI) to detect changes in the lake's water level and surrounding vegetation cover. Raise public awareness and encourage the local community to participate in protecting the lake and its resources and maintaining its ecological balance

References

[1] J.M. Salman, A.J. Mohammed, Exp. Theor. Nanotechnol. 5 (2021) 265 https://doi.org/10.56053/5.2.265
[2] A. I. A. Ali, M. RASHEED, Experimental and Theoretical NANOTECHNOLOGY 10 (2026) 239 https://doi.org/10.56053/10.s.239
[3] Z. S. Ahmed, M. RASHEED, H. S. Ahmed, Experimental and Theoretical NANOTECHNOLOGY 10 (2026) 343 https://doi.org/10.56053/10.s.343
[4] J.H. Azzawi, I.M. Abdulameer, AIP Conf. Proc. 2437 (2022) 0670 https://doi.org/10.1063/5.0092338
[5] Z. S. Ahmed, M. RASHEED, H. S. Ahmed, Experimental and Theoretical NANOTECHNOLOGY 10 (2026) 329 https://doi.org/10.56053/10.s.329
[6] A. Khaleefah, M. RASHEED, Experimental and Theoretical NANOTECHNOLOGY 10 (2026) 289 https://doi.org/10.56053/10.s.289
[7] N. Kadhim, ISPRS Ann. Photogramm. Remote Sens. Spatial Inf. Sci. X-G-2025 (2025) 445 https://doi.org/10.5194/isprs-annals-X-G-2025-445-2025
[8] H.K. Mohammed, M.S. Al-Khafaji, I.A. Alwan, Geosciences 15 (2025) 91 https://doi.org/10.3390/geosciences15010091
[9] H.A. Radeef, I.M. Abdulameer, AIP Conf. Proc. 2769 (2023) 33 https://doi.org/10.1063/5.0150705
[10] A. Titolo, Remote Sens. 13 (2021) 786 https://doi.org/10.3390/rs13040786
[11] M. Rasheed, R. Barillé, Opt. Quantum Electron. 49 (2017) 77 https://doi.org/10.1007/s11082-017-1030-7
[12] H.N. Abbas, I.M. Abdulameer, AIP Conf. Proc. 2307 (2020) https://doi.org/10.1063/5.0027565
[13] M. Fuentealba, Sci. Total Environ. 788 (2021) 147861 https://doi.org/10.1016/j.scitotenv.2021.147861
[14] A. I. A. Ali, M. RASHEED, Experimental and Theoretical NANOTECHNOLOGY, 10 (2026) 277 https://doi.org/10.56053/10.s.277
[15] A. Raghdi, M. Heraiz, M. Rasheed, A. Keziz, Journal of the Indian Chemical Society, 101 (2024) 101413 https://doi.org/10.1016/j.jics.2024.101413
[16] H.M. Ghali, R.Z. Azzubaidi, J. Eng. 27 (2021) 42 https://doi.org/10.31026/j.eng.2021.01.03
[17] S. S. Batros, M. Rasheed, H. K. Aity, A. A. Hatef, T. Saidani, Materials Chemistry and Physics, 355 (2026) 132243 https://doi.org/10.1016/j.matchemphys.2026.132243
[18] M. RASHEED, A. Khaleefah, Materials Chemistry and Physics, 353 (2026) 132112 https://doi.org/10.1016/j.matchemphys.2026.132112
[19] T. Saidani, S. Mokhtari, M. Rasheed, H. Lahmar, M. Trari, Journal of the Indian Chemical Society, 103 (2026) 102499 https://doi.org/10.1016/j.jics.2026.102499
[20] H. K. Aity, M. Rasheed, E. Dhahri, A. A. Hateef, T. Saidani, Journal of Materials Science, 61 (2026) 6226 https://doi.org/10.1007/s10853-026-12241-w
[21] M. Rasheed, SuhaShihab, O. Alabdali, H. H. Hassan, J. Phys. Conf. Ser., 1879 (2021) 032113 https://doi.org/10.1088/1742-6596/1879/3/032113

[22] Areej Adnan Hateef, Essebti Dhahri, M. Rasheed, Habiba Kadhim, Z. Abbas, N. Hassan, Physics and Chemistry of Solid State, 25 (2024) 801 https://doi.org/10.15330/pcss.25.4.801-810
[23] Q. Miao, Sci. Total Environ. 928 (2025) 154575 https://doi.org/10.1016/j.scitotenv.2024.154575
[24] N. Ben Azaza et al., Opt. Mater., 96 (2019) 109328 https://doi.org/10.1016/j.optmat.2019.109328
[25] A.A. Salman, F.K. Mashee, A. Ramahi, I.M. Abdulameer, D.H.M., Exp. Theor. Nanotechnol. 9 (2025) 123 https://doi.org/10.56053/9.2.123
[26] A. Boumezoued, K. Guergouri, Régis Barillé, Rechem Djamil, Mourad Zaabat, M. Rasheed, J. Alloys Compd. 791 (2019) 550. https://doi.org/10.1016/j.jallcom.2019.03.251
[27] A.A. Salman, F.K. Mashee, A. Ramahi, I.M. Abdulameer, D.H.M., Exp. Theor. Nanotechnol. 9 (2025) 123 https://doi.org/10.56053/9.S.123
[28] A.K. Rahman, L.S. Chen, M.I. Al-Khalidi, Exp. Theo. NANOTECHNOLOGY 10 (2026) 115 https://doi.org/10.56053/10.1.109
[29] S.M. Kareem, J.T. Wallace, D.R. Singh, Exp. Theo. NANOTECHNOLOGY 10 (2026) 298 https://doi.org/10.56053/10.S.357